

Electronic and Vibrational Properties of γ -AlH₃

Yan Wang, Jia-An Yan, and M. Y. Chou

School of Physics, Georgia Institute of Technology, Atlanta, Georgia 30332-0430

(Dated: February 1, 2008)

Abstract

Aluminum hydride (alane) AlH₃ is an important material in hydrogen storage applications. It is known that AlH₃ exists in multiply forms of polymorphs, where α -AlH₃ is found to be the most stable with a hexagonal structure. Recent experimental studies on γ -AlH₃ reported an orthorhombic structure with a unique double-bridge bond between certain Al and H atoms. This was not found in α -AlH₃ or other polymorphs. Using density functional theory, we have investigated the energetics, and the structural, electronic, and phonon vibrational properties for the newly reported γ -AlH₃ structure. The current calculation concludes that γ -AlH₃ is less stable than α -AlH₃ by 2.1 KJ/mol. Interesting binding features associated with the unique geometry of γ -AlH₃ are discussed from the calculated electronic properties and phonon vibrational modes. The binding of H-s with higher energy Al- p, d orbitals is enhanced within the double-bridge arrangement, giving rise to a higher electronic energy for the system. Distinguishable new features in the vibrational spectrum of γ -AlH₃ were attributed to the double-bridge and hexagonal-ring structures.

PACS numbers: 71.20.Ps, 63.20.Dj, 61.66.Fn, 61.50.Lt

I. INTRODUCTION

Aluminum hydride AlH_3 (alane) is among the most promising metal hydrides for the hydrogen storage medium, containing a usable hydrogen fraction of 10.1 wt.% with a density of 1.48 g/ml. The enthalpy of the reaction is found to be low, resulting in minimal heat exchange for both charging and discharging reactions. This material is thermodynamically unstable near ambient conditions, but it is kinetically stable without releasing much hydrogen for years. However, extremely high hydrogen pressure (exceeding 25 kbar) is required to achieve charging. The decomposition of AlH_3 occurs in a single step:



How to overcome the kinetic barriers and to find new routes to synthesize AlH_3 for reversibility have been the focus of many research activities recently.

Early studies identified seven polymorphs of AlH_3 : α , α' , β , δ , ε , γ , and ξ .¹ It was suggested experimentally that the α phase is the most stable, followed by the β and γ phases.^{2,3} The decomposition of the γ and β phases is faster than that of α phase. A reaction enthalpy of 7.1 KJ/mol- H_2 and 11.4 KJ/mol- H_2 for γ and α , respectively, is reported.^{2,3} The exothermic transition to the α phase from the γ phase is also reported. Only the α polymorph AlH_3 has been experimentally investigated extensively, including structural characterization,⁴ thermodynamic measurements,^{5,6} and thermal and photolytic kinetic studies.^{6,7,8,9,10,11,12} Theoretical calculations^{13,14,15} of α - AlH_3 from first principles have been performed to study the structural stability and electronic and thermodynamic properties. Limited studies have been conducted on other polymorphs and their properties.

Recently, the crystal structure of γ - AlH_3 is reported by two separate groups using synchrotron X-ray powder diffraction¹⁶ and powder neutron diffraction,¹⁷ respectively. A unique feature of double-bridge bonds involving Al-2H-Al is identified in addition to the normal bridge bond of Al-H-Al as found in α - AlH_3 . In the present study, using density functional theory and the linear response approach, we investigate the electronic properties and phonon spectra for the newly published γ - AlH_3 crystal structure.^{16,17} The phase stability and interesting binding characteristics in γ - AlH_3 are presented and compared with that of α - AlH_3 . The origin of the cohesive energy difference in these two phases is discussed. Distinct phonon vibrational modes arising from the double-bridge and hexagonal ring structures are identified.

II. CALCULATIONAL PROCEDURES

The calculations are based on density functional theory.¹⁸ The Kohn-Sham equations are solved in a plane-wave basis using the Vienna *ab initio* simulation package (VASP).^{19,20} For the exchange-correlation functional, the generalized gradient approximation (GGA) of Perdew and Wang (PW91)²¹ is employed. The electron-ion interaction is described by ultrasoft pseudopotentials (USPP).²² The k space integrals are evaluated using the sampling generated by the Monkhorst-Pack procedure.²³ The calculation for both α - and γ -AlH₃ structures are performed with a k -point mesh of $7 \times 7 \times 7$. The relaxations of cell geometry and atomic positions are carried out using a conjugate gradient algorithm until the Hellman-Feynman force on each of the unconstrained atoms is less than 0.01 eV/Å. The nuclear coordinates are first allowed to relax while the cell volume is fixed at the experimental value. Then simultaneous relaxations of the cell volume, shape and atom coordinates are conducted. For the total energy calculations, the plane-wave energy cutoff is 600 eV. The self-consistent total energy converges to within 10^{-5} eV/cell.

The vibrational properties are studied with density functional perturbation theory within the linear response.²⁴ The dynamical matrices are obtained for a uniform grid of q vectors of $4 \times 4 \times 4$ and $3 \times 3 \times 3$ over the Brillouin zone of α - and γ -AlH₃, respectively. This dynamical matrix is then Fourier-transformed to real space and the force-constant matrices are constructed, which are used to obtain the phonon frequencies. The PWSCF numerical code²⁵ was used in our calculations for the zero-point energies and phonon density of states.

III. RESULTS AND DISCUSSIONS

A. structure and Energetics

The structural characterization from an earlier high-resolution synchrotron X-ray diffraction⁴ study concluded that α -AlH₃ has a rhombohedral lattice of space group $R\bar{3}c$ (No. 167). Recent diffraction experiments^{16,17} determined that γ -AlH₃ has an orthorhombic unit cell with space group $Pnnm$ (No. 58). The unit cell for γ -AlH₃ is shown in Figure 1(a), compared with the hexagonal α -AlH₃ in Figure 1(c). The experimentally reported lattice constants are listed in Table I. The building element for both phases is the AlH₆ octahedron, where one Al atom is surrounded by six H atoms. However, the packing scheme in γ -AlH₃

is more complex than that in α -AlH₃. The AlH₆ octahedra are connected simply by sharing vertices in α -AlH₃, as illustrated in Figure 1(c). The network of these octahedra produces only one type of Al-H-Al bridge bond which has a bond angle and a bond length of 142° and 1.712 Å, respectively. In contrast, in γ -AlH₃ the AlH₆ octahedra are connected not only by sharing vertices as in α -AlH₃, but also by sharing edges, as shown in Figure 1(a). As a consequence, two nonequivalent Al atoms, Al1 and Al2, are created. Four nonequivalent H atoms (H1-H4)¹⁶ are also identified as shown in Figure 1(a), while only one type H atom exists in α -AlH₃. Al1 is involved with the normal bridge bond with H, which is similar to that in α -AlH₃ but with a slight difference in the bond length and angle. However, Al2 involves a new type of double-bridge configuration Al2-2H3-Al2, as shown near the center of unit cell in Figure 1(a). This double-bridge bond gives a smaller distance of 2.60 Å between the two Al2 atom compared with the Al-Al separation of 3.24 Å in α -AlH₃ and 2.86 Å in Al metal. In addition to the new double-bridge configuration, a hexagonal-ring structure is found consisting of two Al2, two Al1, and four H4 atoms, as shown in Figure 1(b). The four Al atoms are on one plane parallel to the c-axis while the H4 atoms have a slight displacement (~ 0.14 Å) out of this plane. These rings are connected to form linear chains along c-axis. The structures of double bridge in the ab-plane and the hexagonal-ring along c-axis are unique to γ -AlH₃ and have not been found in any other hydrogen-containing aluminum compounds. Furthermore, the α phase possesses a higher order of symmetry than that of the γ phase, with a smaller primitive trigonal unit cell. The total number of formula units (f.u.) in a unit cell is six and two for the γ and α phases, respectively. The molecular volume (the density) for the γ phase is found to be higher (lower) than that of the α phase by 11% (10%).

Using the experimentally established space groups and unit cells as shown in Figure 1, the total energies and structural parameters for both the α and γ phases are studied from first-principles calculations. The calculated results for the fully relaxed structures are summarized in Table I. The theoretical lattice parameters are in good agreement with the observed values for both γ - and α -AlH₃ and are consistent with the results from previous α -AlH₃ calculations.^{13,14} The calculated cohesive energies indicate that γ -AlH₃ is energetically less stable than α -AlH₃ by 2.3 KJ/mol, which is in fair agreement with the measured value of 4.3 KJ/mol.^{2,3} In addition, in γ -AlH₃ various bond lengths for non-equivalent Al and H atoms are evaluated and compared with recent experimental results of synchrotron X-

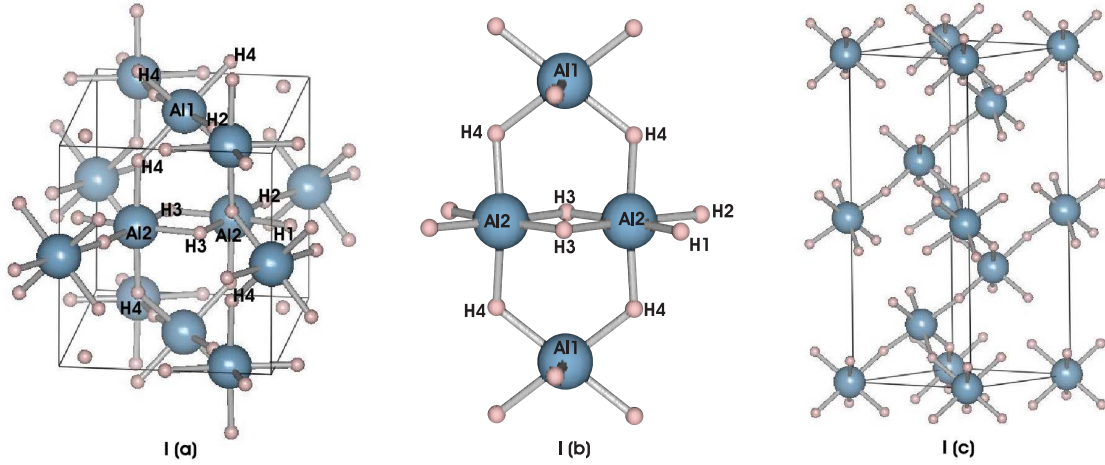


FIG. 1: (Color Online) Crystal structures of (a) orthorhombic γ -AlH₃, (b) hexagonal-ring structure in γ -AlH₃, and (c) hexagonal α -AlH₃. The large and small spheres denote Al and H atoms, respectively.

TABLE I: Calculated cohesive energies and structural parameters for γ -AlH₃ and α -AlH₃ compared with values from experiments and previous calculations.

Configuration	Cohesive Energy		Lattice Parameters				
	eV/(f.u.)	a(Å)	b(Å)	c(Å)	$\alpha(^{\circ})$	$\beta(^{\circ})$	$\gamma(^{\circ})$
α -AlH ₃ :							
Current work	-14.052	4.49	4.49	11.80	90.0	90.0	120.0
Previous work (Ref.13)		4.42	4.42	11.80	90.0	90.0	120.0
(Ref.14)		4.489	4.4489	11.820	90.0	90.0	120.0
Experiment (Ref.4)		4.449	4.449	11.813	90.0	90.0	120.0
γ -AlH ₃ :							
Current work	-14.028	5.43	7.40	5.79	90.0	90.0	90.0
Experiment (Ref.16)		5.3806	7.3555	5.77509	90.00	90.00	90.00
(Ref.17)		5.3672	7.3360	5.7562	90.00	90.00	90.00

ray powder diffraction¹⁶ and powder neutron diffraction¹⁷ in Table II. Good agreements are found between the calculated and observed values. Without including the zero point energy, the calculated reaction enthalpies for equation (1) of α and γ phases are 9.2 and

TABLE II: Interatomic distances (\AA) and bond angles (deg) obtained from the fully relaxed structure of $\gamma\text{-AlH}_3$. The values from the synchrotron X-ray diffraction¹⁶ and the powder neutron diffraction¹⁷ are also included for comparisons.

Bond	Calc.	Ref.16/Ref.17	Bond	Calc.	Ref.16/Ref.17	Angle	Calc.	Ref.16/Ref.17
Al1-Al2	3.18	3.1679/3.155	Al2-H1	1.69	1.668/1.657	Al1-H4-Al2	134.7	124.0/133.88
Al2-Al2	2.62	2.602/2.585	Al2-H2	1.70	1.664/1.678	Al1-H2-Al2	168.8	171.0/169.99
Al1-H2	1.76	1.769/1.764	Al2-H3	1.72	1.70/1.755	Al2-H1-Al2	180.0	180.0/179.99
Al1-H4	1.72	1.784/1.696	Al2-H4	1.72	1.790/1.733	Al2-H3-Al2	97.3	100.7/97.53
			H3-H3	2.30	2.16/2.266	H4-Al1-H4	85.9	76.34/85.00
						H4-Al2-H4	176.3	170.63/176.84

10.8 KJ/mol- H_2 , respectively, which are also consistent with the measured values.^{2,3}

B. Electronic Structure

The electronic structure of the γ - AlH_3 is first analyzed by examining the charge distribution and charge transfer. The difference charge density $\Delta\rho(\mathbf{r})$ is the difference between the total charge density of the solid and a superposition of the atomic charge with the same spatial coordinates as in the solid:

$$\Delta\rho(\mathbf{r}) = \rho_{solid}(\mathbf{r}) - \sum_i \rho_{atom}^i(\mathbf{r} - \mathbf{R}_i), \quad (2)$$

where the sum is over all the atoms. Figure 2 shows such plots in the planes containing two different types of Al-H configurations in $\gamma\text{-AlH}_3$. The solid squares and circles represent Al and H positions, respectively. The (002) plane shown in Figure 2(a) contains one double-bridge bond Al2-2H3-Al2 and two other H atoms (H1 and H2), while the (001) plane shown in Figure 2(b) contains a normal bridge H2-Al1-H2. The difference density plot shows the positive values (solid contours) at the H positions, indicating a charge transfer from Al to H. As a result, aluminum is positively and hydrogen is negatively charged. The maximum of contour lines is in the order of 0.014 electrons/ $(\text{\AA})^3$ for both (a) and (b). The minimum is about -0.002 electrons/ $(\text{\AA})^3$ and the step size of the contours is 0.001 electrons/ $(\text{\AA})^3$. The zero difference charge density line forms a closed contour around H, leaving a negative charge

density in the interstitial regions.

In Figure 2(a), note that the positive contours of difference charge density are not exactly centered at the two H3 sites. The local maximum near each H3 is slightly shifted toward each other and the zero difference charge density line encloses both H3, showing some interactions between the H3 pair. In contrast, this is not seen for other H atoms, nor in the normal H-Al-H structure in α -AlH₃. The separation between two H3 atoms in a double-bridge configuration is 2.3 Å, which is slightly smaller than that of other neighboring H pairs. The distance of the two Al2 atoms (2.62 Å) is also small compared with that in Al metal (2.86 Å). The contour lines in Figure 2(a) also shows enhanced interactions between H-s and Al-d electrons. For comparison, the difference charge density for α -AlH₃ is also calculated and plotted in Figure 3 for the (010) plane containing normal Al-H bonds. It is found that the normal bridge

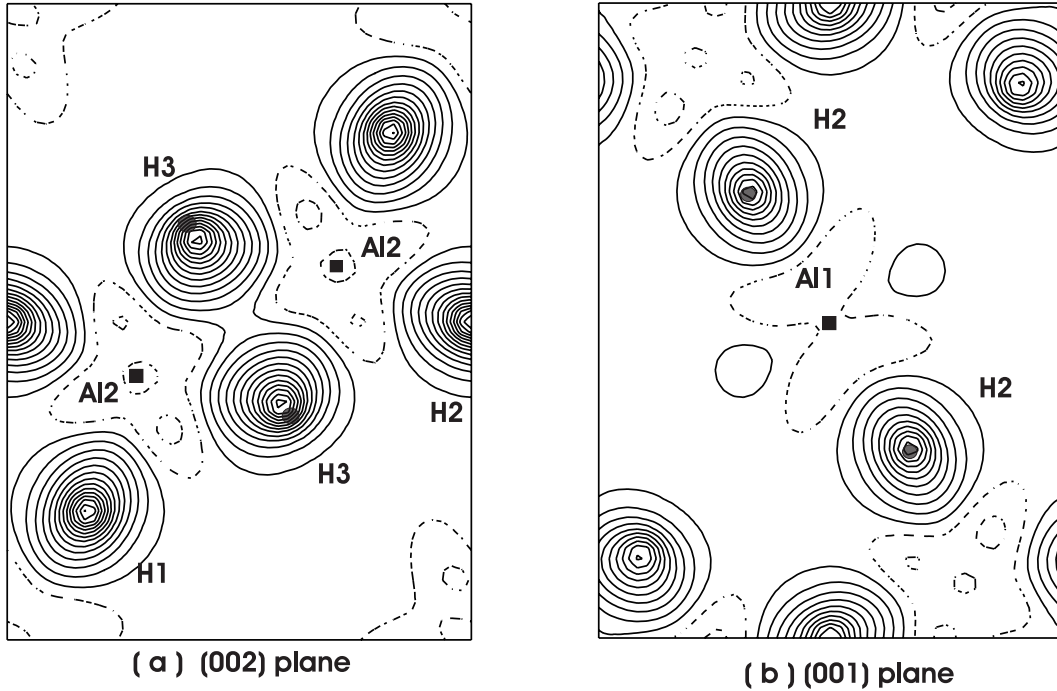


FIG. 2: Difference charge density plots (see text) for γ -AlH₃ in the planes containing Al and H atoms: (a) the (002) plane and (b) the (001) plane. The solid squares and circles represent Al and H positions, respectively. The density contour interval is 0.001 electrons/(Å³). Charge deficiency is represented by dashed lines, while the density increase near the hydrogen atoms is represented by solid lines.

bond in γ -AlH₃ [Figure 2(b)] has similar characteristics as that in α -AlH₃ (Figure 3). The binding between Al and H atoms involves a charge transfer in both α - and γ -AlH₃.

The total electronic densities of states (DOS) for both structures are calculated and given in Figure 4. The projected DOS onto H and Al for α -AlH₃ are also presented in Figure 4.

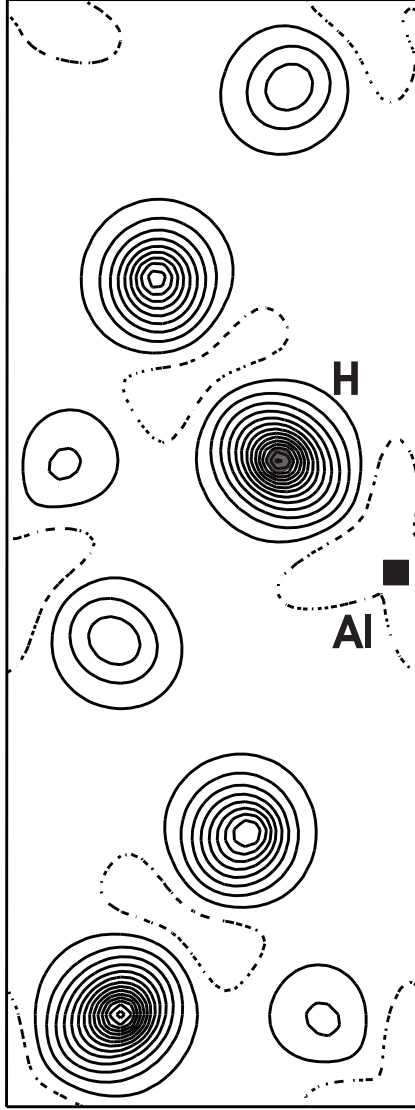


FIG. 3: Charge-density difference plot for α -AlH₃ in a plane containing Al and H atoms. The solid square and circle represent Al and H positions, respectively. The density contours in an interval of 0.001 electrons/(Å³) are presented for the (010) plane. Charge deficiency is represented by dashed lines, while the density increase near the hydrogen atoms is represented by solid lines.

The angular-momentum projected DOS is evaluated by integrating over a sphere centered at each atom with a radius of 1.0 Å for Al and 0.9 Å for H, respectively. The choice of the H radius is based on the charge distribution around H in order to catch the charge transfer to H. The radius of Al is then chosen according to the Al-H bond length in order to cover

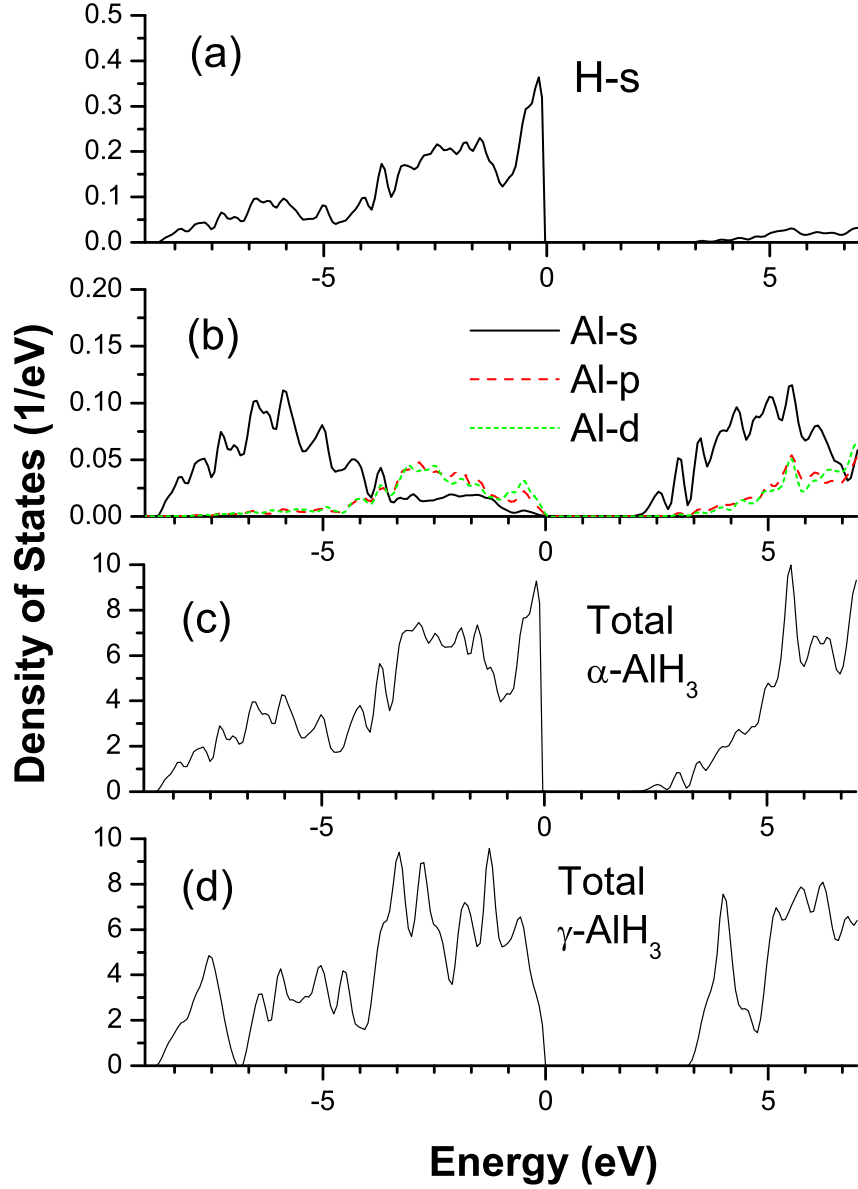


FIG. 4: (Color Online) Calculated electronic density of states (DOS) projected onto (a) H and (b) Al in α -AlH₃, as well as the total DOS for the (c) α -AlH₃ and (d) γ -AlH₃. The Fermi level is at zero.

as much of the interstitial region as possible without overlapping the spheres. The Fermi energy is set to zero in these plots.

The current results for α -AlH₃ are comparable with previous calculations.^{13,14,15} The H-s component spans the whole energy range. The lowest peak from ~ -8.7 to -4.0 eV is found to correspond to H-s and Al-s states, while the higher-energy features are composed of H-s and Al-p or -d states. The total bond width is similar in both α - and γ -AlH₃. A difference between the two is clearly seen near -7 eV, where a small band gap is created in the low

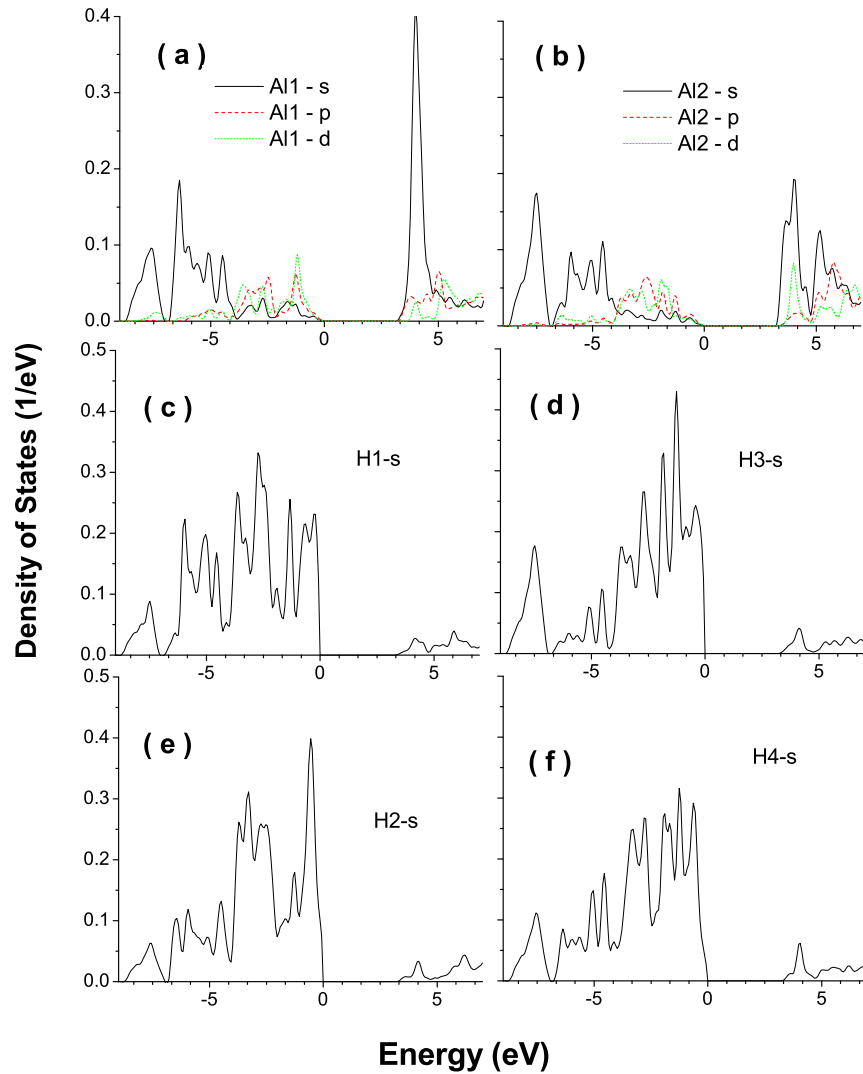


FIG. 5: (Color Online) Calculated electronic density of states projected onto non-equivalent atoms in γ -AlH₃. The Fermi energy is set to be zero.

energy region in γ -AlH₃. This new gap gives rise to a broad, separated DOS peak from -8.7 to -7.0 eV.

In order to understand the new feature found in the DOS of γ -AlH₃, the projected density of states onto non-equivalent Al and H atoms are analyzed in Figure 5. The same radius values used in α -AlH₃ are adopted for integrating over the spheres around Al and H atoms.

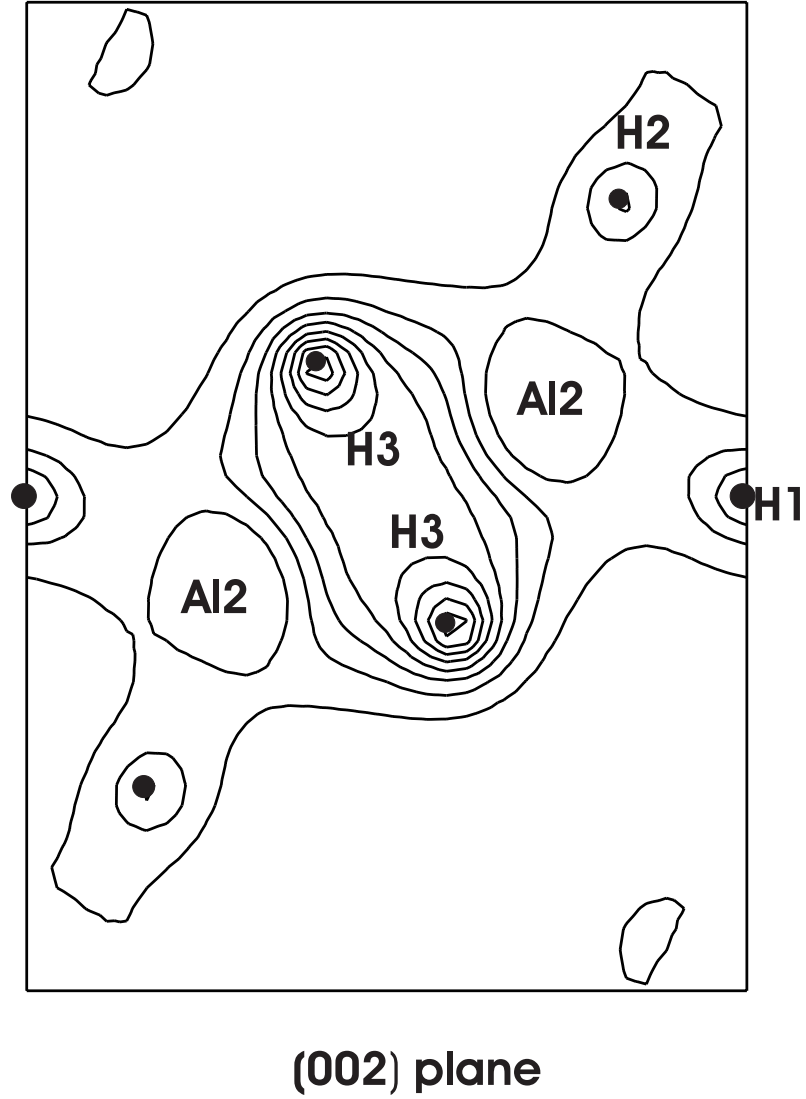


FIG. 6: Total charge density for the lowest two energy bands projected onto the (002) plane, the same plane as shown in Figure 2(a). The solid circles represent H positions. The maximum, minimum and the interval of the contours are 0.85, 0.002, and 0.1 electrons/(Å³), respectively.

The valence states below the Fermi energy can be grouped into three energy regions: the low(-8.7 to -7.0), the middle(-6.8 to -4.0), and the high(-4.0 to 0 eV) energy regions.

The broad peak in the low energy region of -8.7 to -7.0 is composed of considerable

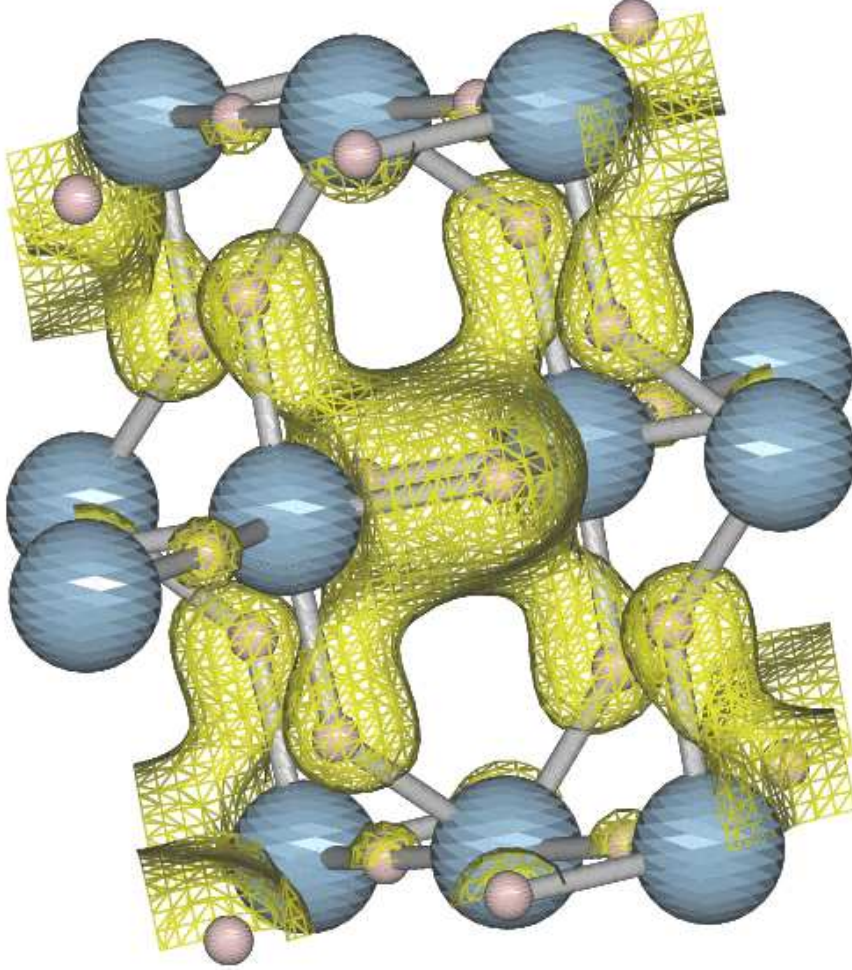


FIG. 7: (Color Online) Total charge density isosurface for the lowest two energy bands in γ -AlH₃. The cell structure is the same as shown in Figure 1(a). The constant charge density surface shown is for 0.45 electrons/(\AA)³. The charge accumulation within the hexagonal-ring structure defined in Figure 1(b) is clearly shown.

H3-s states, with some s contributions from other H and two Al atoms. This broad peak consists of the first two energy bands separated from the other bands at higher energies by a small gap. In Figure 6, the total charge density for these two bands is calculated and plotted for the (002) plane, the same plane shown in Figure 2(a). The maximum, minimum and interval of the contours are 0.85, 0.002, and 0.1 electrons/ $(\text{\AA})^3$, respectively. It shows noticeable charge accumulation around the H3-H3 pair. The three-dimensional isosurface of the total charge density for the same lowest two bands is shown in Figure 7, which has a density value of 0.45 electrons/ $(\text{\AA})^3$. Again, the interaction between the H3-H3 pair is illustrated. In addition, considerable charge is found around four H4 atoms within the same hexagonal-ring as defined in Figure 1(b). Therefore, the broad peak in the low energy region is attributed mainly to the unique double-bridge and hexagonal-ring structures in γ -AlH₃.

In fact, the projected DOS associated with H3 is reduced in the middle energy region (-6.8 to -4.0 eV) compared with other H atoms. The missing amplitude is shifted to both the low (-8.7 to -7.0 eV) and high (-4.0 to 0 eV) energy regions. The former contains an increased H3-H3 interaction, the H-s and Al2-s coupling, while the latter exhibits an enhanced interaction between H3-s and Al2-p and -d states. The stronger interaction of H3-s states with higher-energy Al2-p and -d states due to geometry gives rises to a higher electronic energy for the system.

C. Vibrational Properties

It is expected that the high vibrational frequencies of light hydrogen atoms may result in a significant zero-point energy, which needs to be included in studying the ground-state properties. In order to consider the zero-point energy E_{zpt} contributions to the energetics between the two AlH₃ phases, the phonon density of states (DOS) are evaluated for both α - and γ -AlH₃. Although the absolute value of E_{zpt} is noticeable for the two phases, the difference turns out to be small $\Delta E_{zpt} = E_{zpt}(\alpha) - E_{zpt}(\gamma) = 0.2$ KJ/mol. By including this correction to the total energies previously listed in Table I, the γ phase has a slightly higher energy than the α phase by 2.1 KJ/mol.

The partial phonon density of states (DOS) for atom τ is defined as:

$$\rho_{\tau}(\omega) = \sum_q \sum_{j=1}^{3N} |\mathbf{e}_{\tau}(\mathbf{q}, j)|^2 \delta(\omega - \omega(\mathbf{q}, j)), \quad (3)$$

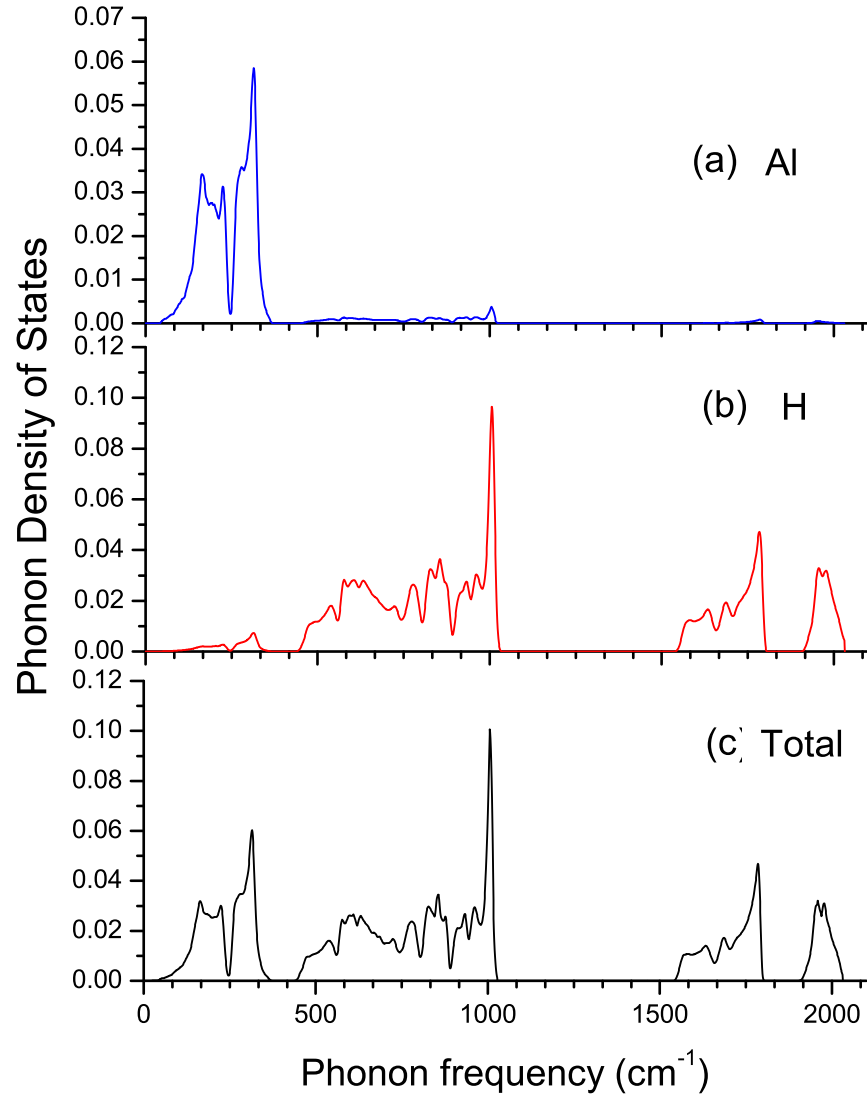


FIG. 8: (Color Online) Total and partial phonon density of states (DOS) for α -AlH₃.

where the N is the total number of atoms per unit cell, \mathbf{q} is the phonon momentum, j labels the phonon branch, $\mathbf{e}_\tau(\mathbf{q}, j)$ is the phonon polarization vector for atom τ , and $\omega(\mathbf{q}, j)$ is the phonon frequency. The total and projected phonon density of states for α - and γ - AlH_3 are

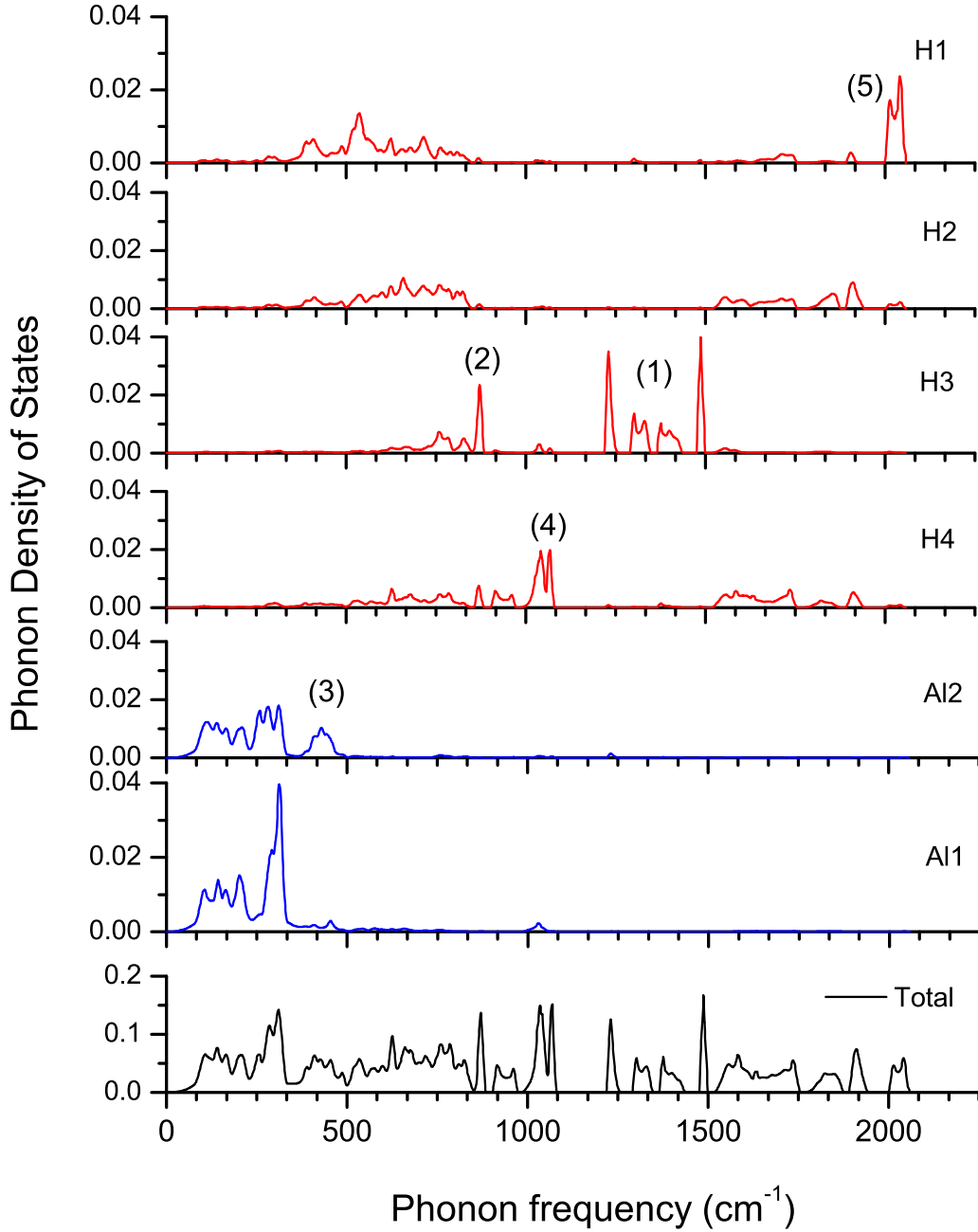


FIG. 9: (Color Online) Total and partial phonon density of states (DOS) for γ - AlH_3 .

presented in the Figures 8 and 9, respectively. Our calculated phonon DOS for α -AlH₃ is in good agreement with previous calculations,^{13,14} showing three distinct groups in the whole frequency range. The decomposed phonon DOS indicates that the low frequency modes below 350 cm⁻¹ are mainly from Al atoms, while the middle and high frequency modes are H- dominated. This is due to the large mass ratio between H atom to Al atom. The high-frequency phonons above 1550 cm⁻¹ are associated with H motion in the Al-H bond stretching modes. No vibrational modes was found in the frequency region from 1025 to 1550 cm⁻¹, yielding gap of 525 cm⁻¹ in α -AlH₃.

The phonon DOS for γ -AlH₃ is more complex than that for α -AlH₃ due to the structural difference. The γ - phase unit cell has much more atoms (24) than the α -phase (8), therefore the calculated phonon DOS for γ -AlH₃ in Figure 9 exhibit more features. Comparing with the phonon DOS of α -AlH₃, although the modes located in the three frequency regions remain, multiple new additional peaks appear in the spectrum. In order to understand how different atomic species contribute to these vibrations, the partial phonon DOS is calculated for the four types of H and two types of Al atoms, as illustrated in Figure 9.

The new features labeled in Figure 9 can be summarized as follows: (1) four new vibrational peaks appear within the gap region of the α -AlH₃ spectrum in the frequency range of 1200 to 1500 cm⁻¹. These are vibrational modes of H3 in the plane of the Al2-2H3-Al2 complex. It consists of both bond stretching and bending motions by H3 on this plane. (2) A new strong narrow peak is introduced in the middle frequency region around a frequency of 875 cm⁻¹, corresponding to the H3 vibrations perpendicular to the Al2-2H3-Al2 plane. (3) An additional broaden peak appears in the low frequency region from 375 to 475 cm⁻¹, which is dominated by Al2 in-plane vibrational modes, coupled with some contributions from H1 and H2 atoms with little contribution from H3. The displacements of the two Al2 atoms have the same magnitude but opposite directions, indicating a paired motion between them. As a consequence, these modes have higher frequencies than the other Al modes. The first three new features are largely related to the motions of the two H3 and the two Al2 atoms in the double-bridge structure. (4) A set of two peaks around 1550 cm⁻¹ are associated with the out-of-plane motion of four H4 atoms in the hexagonal-ring structure shown in Figure 1(b). (5) The set of high-frequency peaks around 2012 cm⁻¹ are associated with H1 atoms which connect two Al2 atoms in opposite directions. The angle Al2-H1-Al2 is 180°. The vibrational modes of H1 are in the *ab* plane and along the Al2-H1-Al2 line.

These new features displayed in the γ -AlH₃ phonon DOS can serve as indicators of these special Al and H arrangements.

IV. CONCLUSION

We have performed pseudopotential density-functional calculations to study the electronic and phonon vibrational properties for the newly reported aluminum hydride γ -AlH₃ structure. The calculated structural parameters are in good agreement with results from the diffraction experiments. Our energetic study for the AlH₃ system indicates that γ -AlH₃ is less stable than α -AlH₃ by ~ 2 KJ/mol. The unique double-bridge configuration in γ -AlH₃ is investigated by examining the electronic properties and phonon vibrational modes. It was found that the double-bridge arrangement modified the binding between H and Al atoms. The projected DOS indicates that interactions exist between the double-bridge H3 atoms and that the interaction between H3-*s* and higher-energy Al2-*p* and -*d* states is enhanced. The latter yields a higher electronic energy in γ -AlH₃. New features in phonon vibrational spectrum associated with double-bridge bonds and hexagonal-ring complex were also identified.

V. ACKNOWLEDGMENT

We thank Dr. V. A. Yartys for bringing Ref. 16 to our attention and stimulating discussions. This work is supported by the Department of Energy under grant No. DE-FG02-05ER46229.

-
- ¹ F. M. Brower, N. E. Matzek, P. F. Reigler, H. W. Rinn, C. B. Roberts, D. L. Schmidt, J. A. Snover, and K. Terada, *J. Am. Chem. Soc.* **98**, 2450 (1976).
 - ² J. Graetz, and J. J. Reilly, *J. Phys. Chem. B* **109**, 22181 (2005).
 - ³ J. Graetz, and J. J. Reilly, *J. Alloys Compds.* **424**, 262 (2006).
 - ⁴ J. W. Turley, H. W. Rinn, and H. J. Fujii, *Inorg. Chem.* **8**, 18 (1968).
 - ⁵ G. C. Sinke, L. C. Walker, F. L. Oetting, and D. R. Stull, *J. Chem. Phys.* **47**, 2959 (1967).
 - ⁶ B. Baranowski, and M. Z. Tkacz, *Phys. Chem.* **135**, 27 (1983).

- ⁷ P. J. Herley, and R. H. Irwin, J. Chem. Phys. Solids **39**, 1013 (1978).
- ⁸ P. J. Herley, O. Christofferson, and R. H. Irwin, J. Chem. Phys. **85**, 1874 (1981).
- ⁹ P. J. Herley, and O. Christofferson, J. Chem. Phys. **85**, 1887 (1981).
- ¹⁰ P. J. Herley, O. Christofferson, and J. A. Todd, J. Solid State Chem. **35**, 391 (1980).
- ¹¹ P. J. Herley, and O. Christofferson, J. Solid State Chem. **85**, 1882 (1981).
- ¹² G. Sandroock, J. Reilly, J. Graetz, W. M. Zhou, J. Johnson, and J. Wegrzyn, J. Appl. Phys. A **80**, 687 (2005).
- ¹³ C. Wolverton, V. Ozolinš, and M. Asta, Phys. Rev. B **69**, 144109 (2004).
- ¹⁴ X. Ke, A. Kuwabara, and I. Tanaka, Phys. Rev. B **71**, 184107 (2005).
- ¹⁵ M. J. van Setten, V. A. Popa, G. A. de Wijs, and G. Brocks, Phys. Rev. B **75**, 035204 (2007).
- ¹⁶ V. A. Yartys, R. V. Denys, J. P. Maehlen, C. Frommen, M. Fichtner, B. M. Bulychev, and H. Emerich, Inorg. Chem. **46**, 1051 (2007).
- ¹⁷ H. W. Brinks, C. Browns, C. M. Jensen, J. Graetz, J. J. Reilly, and B. C. Hauback, J. Alloys Compds. **441**, 364 (2007).
- ¹⁸ P. Hohenberg, and W. Kohn, Phys. Rev. B **136**, B864 (1964); W. Kohn, and L. Sham, Phys. Rev. B **140**, A1133 (1965).
- ¹⁹ G. Kresse, and J. Furthmuller, Phys. Rev. B **54**, 11169 (1996).
- ²⁰ G. Kresse, and J. Furthmuller, Comput. Mater. Sci. **6**, 15 (1996).
- ²¹ J. P. Perdew, J. A. Chewary, S. H. Vosko, K. A. Jackson, M. R. Pederson, D. J. Singh, and C. Fiolhais, Phys. Rev. B **46**, 6671 (1992).
- ²² D. Vanderbilt, Phys. Rev. B **41**, 7892 (1990).
- ²³ H. J. Monkhorst, and J. D. Pack, Phys. Rev. B **13**, 5188(1976).
- ²⁴ S. Baroni, S. Gironcoli, A. Corso, and P. Giannozzi, Rev. Mod. Phys., **73**, 55 (2001).
- ²⁵ PWSCF codes developped by S. Baroni, P. Giannozzi, S. Gironcoli, and Others, www.pwscf.org.